

Seismic linear analytical research on the mechanical effects of RC frame structure under the different column orientations

Mo Shi¹, Min-woo Choi², Yeol Choi³ and Sanggoo Kang⁴

¹Ph.D Candidate, School of Architecture, Kyungpook National University, Korea

²Ph.D Student, School of Architecture, Kyungpook National University, Korea

³Professor, School of Architecture, Kyungpook National University, Korea

⁴Professor, School of Architecture, Kyungpook National University, Korea

<https://doi.org/10.5659/AIKAR.2024.26.3.83>

Abstract The profound impact of earthquakes on human lives and the built environment emphasizes the substantial human and economic losses resulting from structural collapses. Many researchers in this field highlight the long-standing societal challenge posed by earthquakes and underscore the imperative to minimize such losses. Over the decades, researchers have dedicated efforts to seismic design, focusing on improving structural performance to mitigate earthquake-induced damages. This has led to the development of various structural analysis methods. In this research, a specific RC frame structure (401 Bldg.) at Kyungpook National University that is designed for educational purposes, serves as a representative case. This research employs SAP 2000 for simulation, aiming to assess the structural performance under seismic conditions, focusing on evaluating the structural behavior under different column orientations. This research utilizes RSA (Response Spectrum Analysis) to comprehensively examine parameters of displacement, base shear force, base moment, joint radians, and story drift. Referring to the results from RSA, this research also assesses the structural performance using LTHA (Linear Time History Analysis) by conducting synthetic frequency domain and synthetic time domain analyses based on the seismic wave from the Kobe 1995 earthquake (Abeno). Based on the findings from the discussions, this research is expected to be a valuable reference for structural design within seismic resistance and the seismic reinforcement of existing RC frame structures.

Keywords: seismic analysis, RC frame, RSA (Response Spectrum Analysis), LTHA (Linear Time History Analysis), synthetic seismic wave

1. INTRODUCTION

Earthquakes invariably cause significant harm to both people and their surroundings, encompassing economic and human life losses. Numerous researchers are dedicated to understanding each earthquake to minimize both human and economic consequences. In 1995, the Kobe Earthquake struck Japan's second-largest economic region, resulting in approximately 10 trillion yen in economic damages. Such a catastrophic event of this magnitude would undoubtedly have enduring impacts on

the regional economy and surrounding areas. Referring to the research of Yasuhide Okuyama (2014), the impact of recovery and reconstruction activities on the economic structure and interdependence between regions following a catastrophic event was examined.

The research not only investigates economic aspects, but Researchers, including Vanquang Nguyen, Zubair Ahmed Nizamani, Duhee Park, and Ohsung Kwon (2020), also focus on structural damage. Referring to the study on the 1995 Kobe earthquake, the researchers analyze the collapse mechanism of Daikai Station using three-dimensional finite element analyses. Moreover, in the research on the structural damage caused by the 1995 Kobe earthquake of Andi Yusra, Andi Mustafa, Meidia Refiyanni, and Zakia (2023), researchers employ a non-linear pushover approach to analyze building performance under the 1995 Kobe earthquake loads. Using STERA 3D structure analysis software with the 1995 Kobe earthquake spectrum data, the study discusses earthquake response analysis and static response analysis, providing insights into the analyzed building structures' behavior during the seismic event.

Previous research indicates that RSA is computationally efficient and less time-consuming than LTHA. RSA simplifies the seismic analysis process by reducing the complex ground

Corresponding Author: Sanggoo Kang

Professor, School of Architecture, Kyungpook National University, Korea

e-mail: kangs@knu.ac.kr

This is an Open Access article distributed under the terms of the Creative Commons Attribution Non-Commercial License (<http://creativecommons.org/licenses/by-nc/3.0/>) which permits unrestricted non-commercial use, distribution, and reproduction in any medium, provided the original work is properly cited.

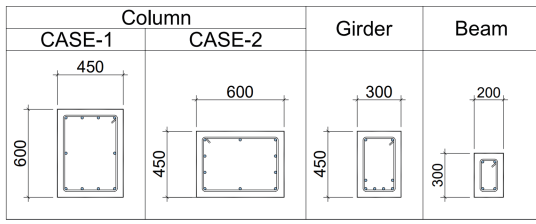


Figure 2. Design of the section of column, girder, and beam

Figure 2 provides a visual representation of the design distinctions among columns sharing the same cross-sectional area of 270,000mm². The columns are divided into two cases: CASE-1, characterized by dimensions of 450mm × 600mm, and CASE-2, featuring dimensions of 600mm × 450mm. In each column section, there are ten longitudinal rebars, specifically D19, accompanied by hoop rebars, D10, spaced at 300mm intervals. Adhering to the standards outlined in KDS 14 20 50 : 2022, the concrete covering depth is maintained at 40mm.

Columns serve as the vertical load-bearing elements that provide essential support to the structure, girders play a crucial role in supporting the structure horizontally, and beams integrate into the entirety of the RC frame structure along the vertical axis. The design of the girders, especially along the corridor forms an enveloping framework that contributes to the overall stability and load distribution of the building. Moreover, the design of beams signifies their crucial role in transferring loads and reinforcing the structural integrity of the building.

The concrete used in this research adheres to the standards set by KS F 4009 : 2021 for ready-mixed concrete. Following the design guidelines for educational buildings in the 1980s from the Republic of Korea’s Ministry of Education, the specified compressive strength is denoted as $F_{ck}=15.12\text{MPa}$, with an anticipated compressive strength of $F_{ek}=18.14\text{MPa}$, as detailed in Table 1.

Table 1. Design of column girder, and beam

· Concrete (C15)	Weight per unit volume	23540 N/m ³
	Mass per unit volume	2400 kg/m ³
	Modulus of elasticity	22334 MPa
	Poisson ratio	0.1667
	Coefficient of Thermal expansion	1.100E-05
	Specified Compressive Strength	15.12 MPa
	Expected Compressive Strength	18.14 MPa
· Rebar (SD300)	Weight per unit volume	77000 N/m ³
	Mass per unit volume	7850 kg/m ³
	Modulus of elasticity	200000 MPa
	Poisson ratio	0.3
	Coefficient of Thermal expansion	1.170E-05
	Minimum Stress	240 MPa
	Expected Stress	300 MPa
· Column	Longitudinal Rebar	8-D19 & 2-D16
	Hoop Rebar	D10@300
· Girder	Longitudinal Rebar	8-D16
	Hoop Rebar	D10@300
· Beam	Longitudinal Rebar	4-D16
	Hoop Rebar	D10@300

Design Source: Structural Design of the 401 Bldg. (KNU)

Reference: Structural design of Yeongcheon Elementary School

Reference: KDS 14 20 50 : 2022 / KS F 4009 : 2021 / KS D 3504 : 2021

In accordance with the guidelines outlined in KS D 3504 : 2021 for steel bars used in concrete reinforcement, and drawing from the educational building design specifications of the 1980s by the Republic of Korea’s Ministry of Education, the strength of the rebar is designated as $F_y=240\text{MPa}$ in Table 1. Additionally, the anticipated stress is designed to be $F_{ey}=300\text{MPa}$.

In accordance with the design principles reminiscent of typical school buildings from the 1980s, and referring to Table 5.3.1 in KISTEC 2021, the shear and moment stiffness values for column and beam sections are specified. For the column section, the shear stiffness is set at 0.45, and the moment stiffness is designated as 0.7. In contrast, for the beam section, the shear stiffness is defined as 0.45, and the moment stiffness is set at 0.35.

(3) Load Description

The Dead Load and Live Load specifications for the educational usage structure of the school building, detailed in Table 3.2-1 of KDS 41 10 15 : 2019, allocate values of 4.3kN/m² and 3kN/m², respectively. Specifically, the Live Load on the corridor is designed to be 4.0kN/m². Additionally, for the roof load considerations, a snow load of 0.5kN/m² is taken into account.

Subsequently, by taking into account the dimensions of each room of the specific RC frame structure, the calculations for the Dead Load, Live Load, and Snow Load can be performed using the formulas provided below:

$$\omega_p = \frac{P_D}{L} \tag{1}$$

$$\omega_L = \frac{P_L}{L} \tag{2}$$

where P_D represents the Dead Load force, and ω_D signifies the uniform load from the Dead Load. Conversely, P_L denotes the Live Load force, and ω_L represents the uniform load from the Live Load. L in both equations represents the length of the girder or beam in this specific RC frame structure. Utilizing these calculations, the Dead Load, Live Load, and Snow Load can be calculated.

(4) Approaches of RSA

The research outlines the analysis of the target structure using the response spectrum methodology based on KISTEC 2021. This involves employing the response spectrum illustrated in Figure 3, derived from KDS 41 17 00 : 2022. Figure 3 also from KDS 41 17 00 : 2022, displays the earthquake hazard map of the Republic of Korea, guiding the definition of the response spectrum for site class S4. This classification is determined by the specific location of the target building of this research, No.401, situated at Kyungpook National University’s Department of Architectural Engineering in Daegu Metropolitan City. The right side of Figure 3 illustrates the corresponding response spectrum for the S4 classification.

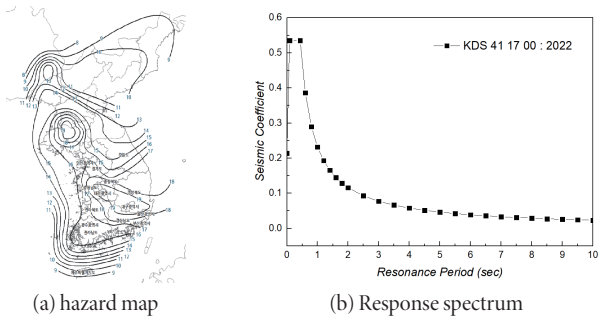


Figure 3. Earthquake hazard map and Response spectrum

The calculation of spectral accelerations is a critical step in seismic analysis. The equations provided by KDS 41 17 00 : 2022 offer a methodological framework for computing these accelerations, taking into account the specific seismic characteristics relevant to the structural assessment. The 1-sec spectral acceleration and the 0.2-sec spectral acceleration are fundamental parameters in understanding how a structure responds to seismic forces over different time intervals. This computational process aids in quantifying the magnitude of ground motion and its impact on the target structure, contributing to a comprehensive seismic analysis in accordance with established standards and methodologies. Utilizing the equations provided by KDS 41 17 00 : 2022, the computation of both the 1-sec spectral acceleration and the 0.2-sec spectral acceleration can be calculated by the following equations:

$$S_{D1} = S \times F_v \times \frac{2}{3} \tag{3}$$

$$S_B = S \times 2.5 \times F_a \times \frac{2}{3} \tag{4}$$

where S represents the effective ground acceleration value for a 2400-year return period earthquake, sourced from KDS 41 17 00 : 2022. Additionally, the factors F_a and F_v , found in Table 4.2-1 and Table 4.2-2 respectively as per KDS 41 17 00 : 2022, play a role. Using these parameters, the calculations yield S_{D1} for the 1-sec spectral acceleration and S_{DS} for the 0.2-sec spectral acceleration. Applying the provided equations, the 1-sec spectral acceleration is computed as 0.22g, while the 0.2-sec spectral acceleration stands at 0.55g. These results are also visually represented on the right side of Figure 3.

(5) Approaches of LTHA

The research mentions the utilization of recorded data on the seismic wave of the Kobe 1995 earthquake, specifically obtained from Abeno on the 16th of January 1995. The data consists of 14,000 recorded points at intervals of 0.01 seconds. The Acceleration and Time results of this specific Response Spectrum are presented in Figure 4.

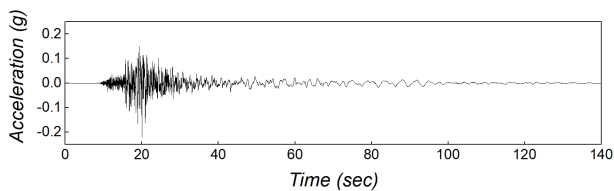
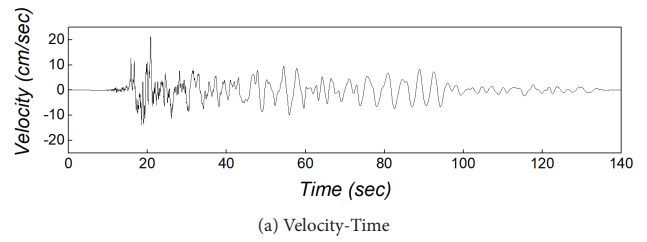
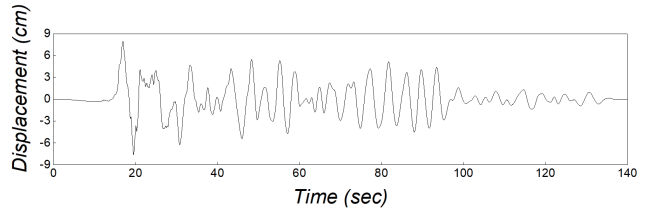


Figure 4. Seismic wave of Kobe 1995 earthquake (Abeno)



(a) Velocity-Time

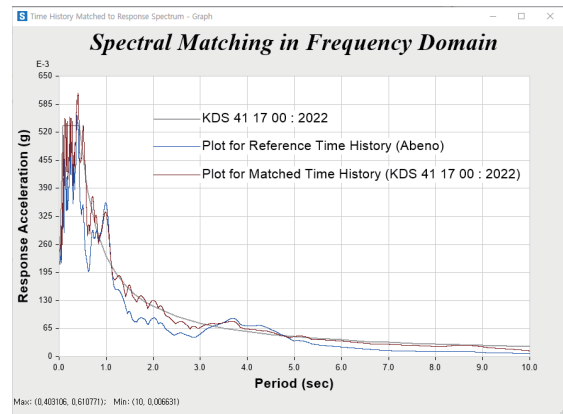


(b) Displacement-Time

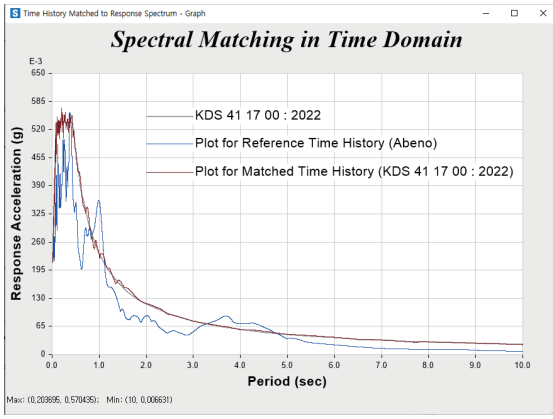
Figure 5. Analytical result of Kobe 1995 earthquake in Abeno

Regarding the discussion of the seismic wave of the Kobe 1995 earthquake, referencing Figure 4, the Acceleration-Time data obtained from the Response Spectrum of the Kobe 1995 earthquake (recorded in Abeno on January 16, 1995) is used to derive analytical results for Velocity-Time and Displacement-Time, as depicted in Figure 5. The analysis extends beyond just seismic acceleration to provide insights into the temporal evolution of velocity and displacement during the seismic event.

The results indicate a comparative analysis of Acceleration-Time, Velocity-Time, and Displacement-Time results. It highlights that the maximum values for velocity and displacement occur in the period from 15s to 20s. This phenomenon is explained by examining the Acceleration-Time results of the Kobe 1995 earthquake in Abeno, where the acceleration peaks at 0.14866g at 19.49s in the positive direction and -0.22063g at 20.04s in the negative direction. The maximum velocity is observed at 21.2488 cm/s at 20.83s in the positive direction and -13.94579 cm/s at 18.49s in the negative direction. Additionally, referring to the result of the Displacement-Time, the maximum displacement values are 79.769mm at 16.92s, and -76.2287mm at 19.52s in the negative direction.



(a) Synthetic Frequency



(b) Synthetic Time

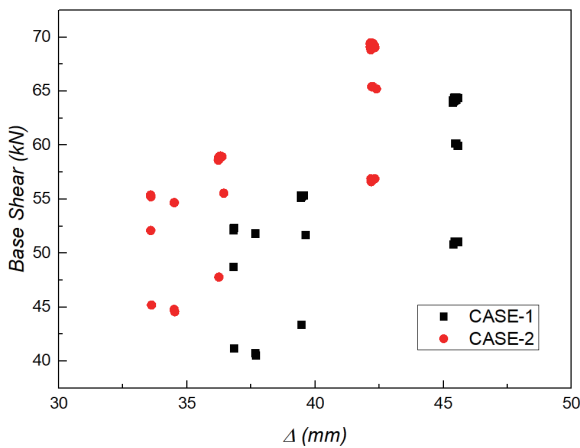
Figure 6. Approaches of LTHA

This research describes the utilization of RSA (Response Spectrum Analysis) and LTHA (Linear Time-History Analysis) to generate a synthetic time history that matches the reference acceleration time history data of the Kobe 1995 earthquake from Abeno. This synthetic time history is created in both the frequency domain and time domain, aligning with the target response spectrum specified in KDS 41 17 00 : 2022. The process is carried out using SAP 2000, as illustrated in Figure 6. The analytical direction of x and y is employed to assess the performance of the specific target RC frame structure, facilitating a comparison of the influences between two different column orientations.

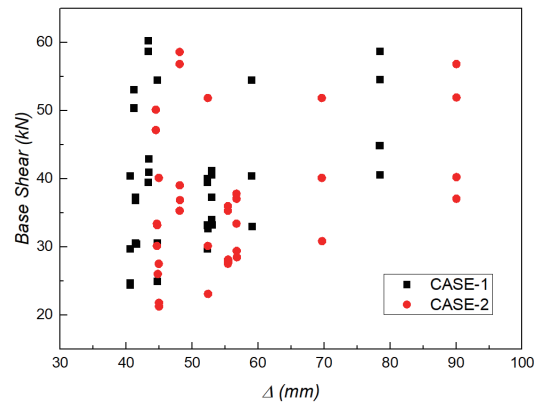
3. DISCUSSION

(1) RSA (Response Spectrum Analysis)

Through the deformed shape of the target RC frame structure under SAP 2000 analysis, it is observed that although larger structural displacements from higher components may cause increased stress, the results still indicate that the structure satisfies the structural safety requirements under RSA. This conclusion is based on the properties of concrete and rebar shown in Table 1.



(a) Direction x

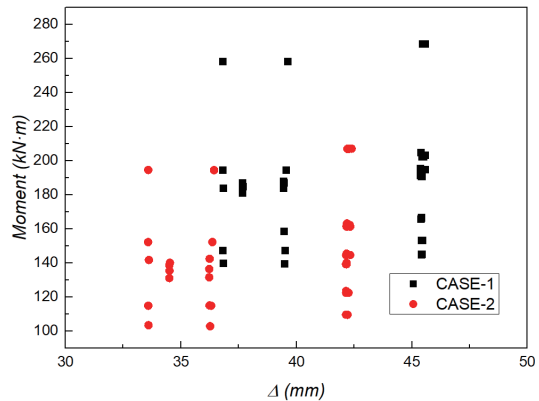


(b) Direction y

Figure 7. Base Shear and Displacement (RSA)

In the specific RC frame structure studied, there are 66 monitored points on both the foundation and the roof. The base shear force values from all 66 foundation points are collected, and the results are separately analyzed in the x and y directions, as depicted in Figure 7. Similarly, 66 monitored points on the roof are used to track the displacement of the structure, with the results showcased in Figure 7. This figure illustrates the relationship between base shear force on the foundation and displacement on the roof, with distinct visualizations for the x and y directions on the topside and underside, respectively.

Referring to the findings from Figure 7, indicate that in CASE-1, along with the load direction, longer column sections result in greater displacement but smaller base shear force compared to CASE-2. Conversely, in the y-direction, CASE-1 shows a slightly larger base shear force and shorter displacement than CASE-2. Combining results from both x and y directions, the study concludes that longer column sections aligned with the load direction exhibit superior performance, characterized by higher reaction forces, larger base shear, and shorter displacements. Conversely, shorter column sections in the load direction exhibit lower reaction forces, smaller base shear, and shorter displacements. The overall trend suggests that longer column designs aligned with the load direction can withstand longer displacements compared to shorter designs in the same direction.



(a) Direction x

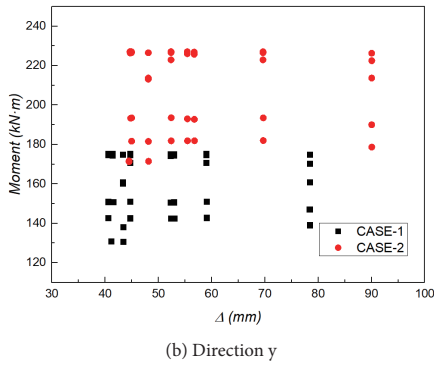


Figure 8. Base Moment and Displacement (RSA)

In Figure 8, graph (a) indicates a larger moment value in CASE-1 in the x-direction, while graph (b) shows a smaller moment value in CASE-1 in the y-direction. Similar to the findings related to base shear and displacement, the results for base moment and displacement reinforce that longer column sections aligned with the load direction exhibit superior performance, characterized by higher moment values. Conversely, shorter column sections aligned with the load direction exhibit lower moment values. This directional discrepancy underscores the structural sensitivity to column length in response to seismic forces. Building upon the discussion of base shear and displacement, the results for base moment and displacement align to affirm the superiority of longer column sections in the load direction. The higher moment values observed in longer column designs suggest an increased capacity to resist bending forces during seismic events. Conversely, shorter column sections in the load direction demonstrate lower moment values, indicating reduced resistance to bending forces.

Many previous studies mention the significance of the story drift in structural performance analysis under seismic loads. This research at hand collects data from 66 monitored points for each story and uses Figure 9 to illustrate the average story drift in both the x and y directions.

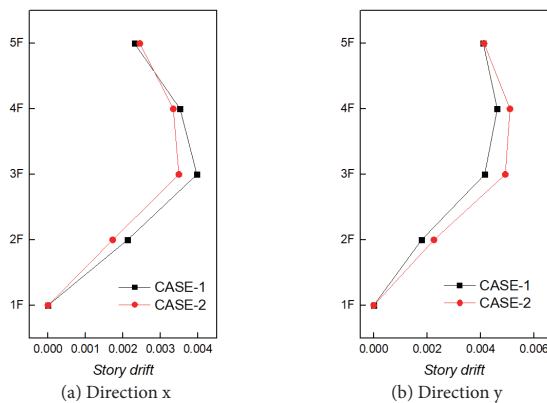


Figure 9. Story drift (RSA)

The story drift is a critical parameter in seismic analysis as it provides insights into how individual layers within a structure respond to seismic forces. By considering 66 monitored points for each story, the research ensures a comprehensive analysis,

capturing variations across the structure. Figure 9 is a crucial visual representation, presenting the average story drift in both the x and y directions. The inclusion of data from multiple points ensures a nuanced understanding of how various parts of the structure contribute to the overall displacement angle.

The analysis regarding the average story drift discusses the findings related to the average story drift in different cases and load directions. In the x direction, CASE-1 exhibits a larger story drift, while in the y direction, CASE-2 shows a larger story drift, as illustrated in Figure 9. This phenomenon underscores the substantial impact of varying column section designs on the RC frame's performance. Specifically, longer column sections aligned with the load direction result in smaller story drift, whereas shorter column sections lead to larger story drift. Additionally, the intersection trend observed in the analysis emphasizes the significant influence of the number of stories on the story drift in the RC frame structure.

The average story drift is a critical parameter in seismic analysis, providing insights into how individual layers within a structure rotate or deform during seismic events. The observed differences between CASE-1 and CASE-2, as well as the variation between the x and y directions, highlight the sensitivity of the structure's response to design choices. The results suggest that the length and orientation of column sections play a pivotal role in influencing the story drift. The choice between longer and shorter column sections can have a significant effect on the structure's ability to withstand seismic forces and the intersection trend related to the number of stories further emphasizes the complex interplay of design factors in determining the story drift.

(2) LTHA (Linear Time History Analysis)

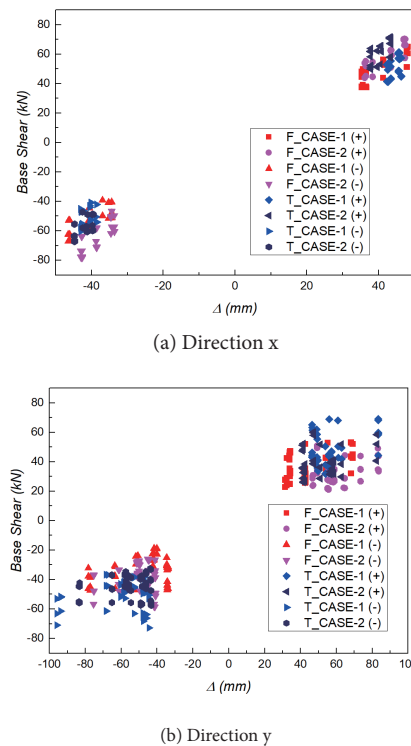


Figure 10. Base Shear and Displacement (LTHA)

Referring to the deformed shape of the target RC frame structure under LTHA, the results illustrate that larger structural displacements from higher components may cause increased stress. However, based on the concrete and rebar properties presented in Table 1, regardless of the synthetic approach, whether in the frequency domain or time domain, the results indicate that the structure is satisfied with structural safety requirements under LTHA.

The research also discusses the significance of linear time-history analysis in seismic performance research, specifically in the context of a study on the Kobe 1995 earthquake. In this research, LTHA is employed based on the seismic wave of the Kobe 1995 earthquake in Abeno. The synthetic response spectrum is generated through a response spectrum synthetic approach in SAP 2000, aligning with KDS 41 17 00 : 2022. Unlike RSA, LTHA introduces positive and negative zones, and eight different analytical data sets are derived using spectral matching methods in both the frequency and time domains, as depicted in Figure 10.

Linear time-history analysis is a crucial tool for evaluating the seismic behavior of structures. In the context of this research, the approach is tailored to the characteristics of the seismic wave of the Kobe 1995 earthquake in Abeno, providing a dynamic understanding of the structure’s response. The synthetic response spectrum is a key element, as it captures the earthquake’s impact on the structure over time, and the alignment with KDS 41 17 00 : 2022 ensures that the analysis conforms to relevant seismic design standards. Comparing LTHA with RSA, the inclusion of positive and negative zones in LTHA offers a more comprehensive perspective on the structural response. The analysis involves 66 monitored points on both the foundation and the roof of the specific RC frame structure, allowing for a detailed examination of base shear force values and displacement. Figure 10 presents the results, showcasing the correlations in the structure’s behavior during seismic events. Also, the eight different analytical data sets derived from spectral matching in the frequency and time domains contribute to a valuable insight into the structure’s response.

The results of base shear and displacement in Figure 10 discuss the comparative analysis of different column orientation designs, specifically focusing on CASE-1 and CASE-2. In terms of the direction x, CASE-2 demonstrates a larger base shear force compared to CASE-1, as illustrated in graph (a) of Figure 10. Conversely, CASE-1 exhibits a slightly longer displacement than CASE-2 in the same direction of the analysis. Additionally, the discrepancy in results becomes more evident when considering the direction y. The analytical data reveals that, in this direction, CASE-1 surpasses CASE-2 in both having a larger base shear and a shorter displacement. This contrast with the direction x analysis highlights the sensitivity of the structural response to different column orientation designs. Moreover, these findings are consistent across both spectral matching approaches in the frequency domain and time domain, providing a robust validation of the results.

The discussion regarding the results of the base moment and displacement sheds light on the influences of different column orientation designs with identical section areas. Figure

11 visually represents these results, emphasizing the nuanced relationship between the structural configurations of CASE-1 and CASE-2. In the analysis of the base moment, graph (a) of Figure 11 illustrates that CASE-1 exhibits a larger base moment when considering the direction x. Conversely, in the analysis of direction y, graph (b) of Fig. 18 indicates that CASE-2 demonstrates a larger base moment. This divergence in results also emphasizes the sensitivity of the structural response to the orientation of the analysis. Furthermore, the discussion draws parallels to the relationship between base shear and displacement, emphasizing the consistency of results across different synthetic methods. Two distinct approaches (Frequency Domain and Time Domain), namely the seismic wave by the Kobe 1995 earthquake (Abeno) in the frequency domain and time domain, yield identical results in the analysis of base moment and displacement, as depicted in Figure 11.

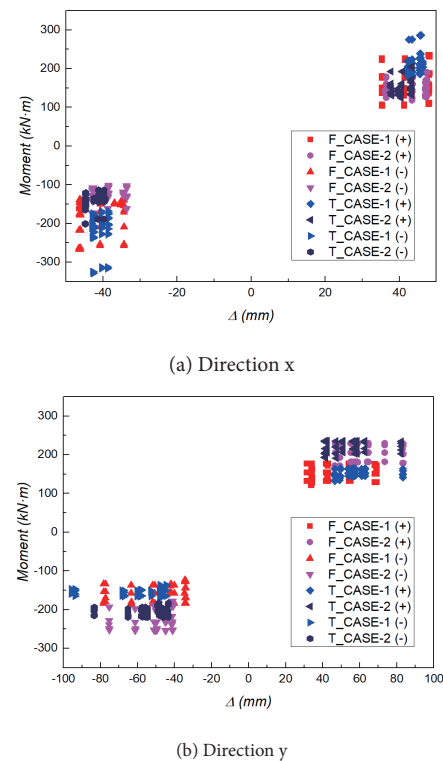


Figure 11. Base Moment and Displacement (LTHA)

The results from Table 2 to Table 5 underscore the importance of displacement and radians analysis as crucial methods for evaluating structural performance under seismic conditions. It further notes that the results of displacement and radians under linear time-history analysis are similar to those obtained from response spectrum analysis. Referring to Table 2 and Table 3, in the x-direction, CASE-1 exhibits a longer average displacement, while in the y-direction, CASE-2 demonstrates a longer average displacement. Referring to Table 4 and Table 5, depicting radians by different stories, indicate that larger radians are observed in CASE-1 for the x-direction, and larger radians are seen in CASE-2 for the y-direction. In summary, the data consistently reveal that longer displacements are associated with larger radians, while shorter displacements align with smaller radians. This pattern holds true for both design cases.

Table 2. Displacement (Frequency domain)

• Stories	CASE-1		CASE-2	
	Direction-x mm	Direction-y mm	Direction-x mm	Direction-y mm
• 1F (+)	0.00	0.00	0.00	0.00
• 2F (+)	7.64	5.28	6.81	8.32
• 3F (+)	21.94	17.53	20.59	26.52
• 4F (+)	34.62	31.21	33.79	45.36
• 5F (+)	42.93	43.36	43.47	60.60
• 1F (-)	0.00	0.00	0.00	0.00
• 2F (-)	-7.45	-5.79	-6.17	-7.07
• 3F (-)	-21.39	-19.28	-18.65	-22.53
• 4F (-)	-33.75	-34.39	-30.60	-38.55
• 5F (-)	-41.85	-47.86	-39.35	-51.53

Table 3. Displacement (Time domain)

• Stories	CASE-1		CASE-2	
	Direction-x mm	Direction-y mm	Direction-x mm	Direction-y mm
• 1F (+)	0.00	0.00	0.00	0.00
• 2F (+)	7.43	7.12	6.15	8.30
• 3F (+)	21.83	23.29	18.94	25.23
• 4F (+)	35.21	41.45	31.62	41.67
• 5F (+)	44.38	57.94	41.24	54.79
• 1F (-)	0.00	0.00	0.00	0.00
• 2F (-)	-7.25	-7.17	-6.55	-7.86
• 3F (-)	-20.94	-23.76	-19.94	-24.59
• 4F (-)	-33.18	-42.27	-32.92	-41.78
• 5F (-)	-41.22	-58.78	-42.66	-56.51

Table 4. Radians (Frequency domain)

• Stories	CASE-1		CASE-2	
	Direction-x rad	Direction-y rad	Direction-x rad	Direction-y rad
• 1F (+)	0.00000	0.00000	0.00000	0.00000
• 2F (+)	0.00297	0.00310	0.00346	0.00306
• 3F (+)	0.00414	0.00343	0.00447	0.00366
• 4F (+)	0.00402	0.00256	0.00398	0.00299
• 5F (+)	0.00343	0.00154	0.00307	0.00207
• 1F (-)	0.00000	0.00000	0.00000	0.00000
• 2F (-)	-0.00270	-0.00302	-0.00407	-0.00277
• 3F (-)	-0.00375	-0.00334	-0.00526	-0.00332
• 4F (-)	-0.00363	-0.00250	-0.00467	-0.00270
• 5F (-)	-0.00308	-0.00150	-0.00360	-0.00188

Table 5. Radians (Time domain)

• Stories	CASE-1		CASE-2	
	Direction-x rad	Direction-y rad	Direction-x rad	Direction-y rad
• 1F (+)	0.00000	0.00000	0.00000	0.00000
• 2F (+)	0.00367	0.00306	0.00379	0.00280
• 3F (+)	0.00507	0.00353	0.00488	0.00346
• 4F (+)	0.00494	0.00277	0.00461	0.00293
• 5F (+)	0.00425	0.00173	0.00371	0.00210
• 1F (-)	0.00000	0.00000	0.00000	0.00000
• 2F (-)	-0.00361	-0.00295	-0.00395	-0.00296
• 3F (-)	-0.00499	-0.00330	-0.00479	-0.00358
• 4F (-)	-0.00498	-0.00248	-0.00439	-0.00302
• 5F (-)	-0.00435	-0.00150	-0.00359	-0.00216

Furthermore, insights from the earlier discussion on RSA emphasize the interplay between base shear, base moment, and displacement, highlighting the significant impact of different column orientation designs on the RC frame's performance. The detailed results in Tables 2, 3, 4, and 5 provide a comprehensive overview of how displacement and radians vary under the influence of different synthetic methods.

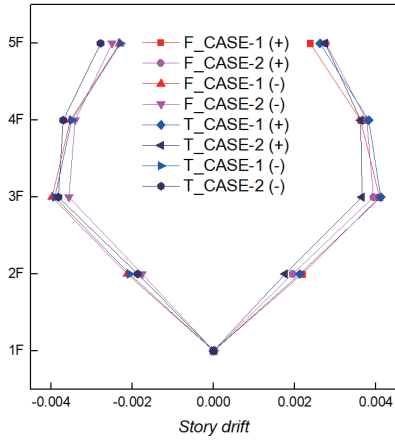
The specific values in the tables above illuminate the performance of the RC frame structure, shedding light on the impact of seismic forces on both displacement and rotational behavior. These findings reinforce the notion that the length of displacements and the magnitude of radians are closely tied. Longer displacements, indicative of more substantial structural movement, correspond to larger radians, signifying greater rotational effects. Conversely, shorter displacements coincide with smaller radians, suggesting limited rotation during seismic events. This consistent relationship between displacement and radians across different synthetic methods underscores the robustness of the observed trends.

Specifically, longer column sections, when aligned with the load direction, exhibit superior performance, characterized by larger base shear, shorter displacements, and smaller radians. Conversely, shorter column sections aligned with the load direction display smaller base shear, shorter displacements, and larger radians. The conclusion drawn is that longer designs, aligned with the load direction, have the capacity to withstand longer displacements compared to shorter designs in the same direction.

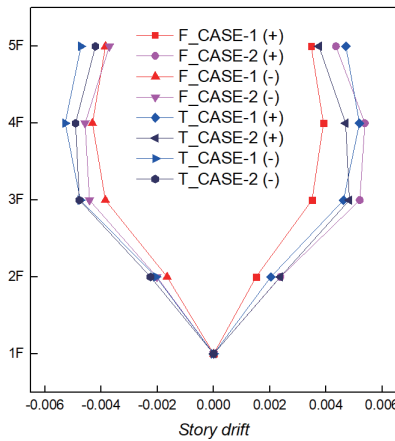
Regarding the average story drift in LTHA in comparison to RSA. Figure 12 presents the results of positive and negative average story drift for the specific RC frame structure based on LTHA using synthetic response spectrum characteristics. Graph (a) of Figure 12 illustrates the average story drift in the x direction. In this analysis, CASE-1 generally exhibits a larger story drift than CASE-2 basically. However, an intersection appears between the 3rd to 5th floors. This intersection aligns with observations made during RSA, indicating a consistent trend across different seismic analysis methods. Conversely, when examining the average story drift in the y direction (Graph (b) of Figure 12), CASE-2 demonstrates a larger story drift than CASE-1. In this situation, the intersection points are more pronounced, highlighting a clearer trend compared to the x-direction results. The presence of intersection points in both directions suggests an influence of column orientation designs on the story drift. However, it's noteworthy that the synthetic response spectrum based on the time domain reveals more distinct intersection points than the frequency domain counterpart. This observation implies that the temporal characteristics of seismic forces have a more pronounced effect on the story drift than frequency-based characteristics.

To summarize the results between story drift obtained through RSA (Response Spectrum Analysis) and LTHA (Linear Time History Analysis). Both analyses reveal that longer column sections aligned with the load direction contribute to smaller story drift, while shorter column sections result in larger story drift. Moreover, the observed intersection trend in the analysis further underscores the impact of the number of stories on the story drift in the RC frame structure. This implies that the

building’s vertical dimension, represented by the number of stories, plays a significant role in influencing how seismic forces manifest in terms of story drift. The intersection trend suggests that certain story levels may experience variations in the story drift based on the interaction between structural characteristics and seismic input.



(a) Direction x



(b) Direction y

Figure 12. Story drift (LTHA)

In practical terms, these findings imply that the choice of column section orientation and the overall height of the structure are crucial factors in determining how the structure responds to seismic forces. Longer column sections, aligned with the load direction, not only result in smaller story drift but also contribute to a more favorable seismic performance. Conversely, shorter column sections may lead to larger story drift, potentially impacting the structural response during seismic events. In summary, the results indicate that the choice of column section orientations has a substantial impact on the average story drift, influencing the structure’s response to seismic forces.

4. CONCLUSION

This research focuses on the seismic analysis of a typical

educational RC frame structure at Kyungpook National University, employing two methods: RSA (Response Spectrum Analysis) and LTHA (Linear Time History Analysis). The goal is to evaluate structural performance under seismic forces with different column orientations, allowing for a detailed examination of how different column configurations influence seismic performance.

The conclusion of this research emphasizes the significant impact of different column orientations on the performance of an RC frame structure, as analyzed through RSA and LTHA. Longer column sections aligned with the load direction consistently demonstrate superior performance across various parameters. The results, particularly concerning base shear force, base moment, and displacement, indicate that longer column sections exhibit larger base shear and base moment, coupled with shorter displacements.

Moreover, the analytical results of average story drift, average displacement, and radians are also discussed. The findings reiterate that longer column sections aligned with the load direction exhibit superior characteristics, including smaller story drift and shorter displacements. This suggests that such configurations can withstand larger radians under seismic conditions. Additionally, the discussion highlights a noteworthy intersection from the 3rd floor to the 5th floor of the specific RC frame structure, particularly in the analysis of radians and average story drift. This intersection underscores the complexity of the structural analysis, indicating that specific story heights or structural elements contribute to variations in joint radians. As a result, the conclusion drawn from the analysis emphasizes the substantial influence of the number of stories on the radians of the joints in the RC frame structure.

To discuss a comparison between two approaches for synthesizing response spectrum—frequency domain and time domain—based on LTHA (Linear Time History Analysis). The strong correlation observed in the results of 66 different monitored points for base shear and base moment by the time domain indicates that the synthetic response spectrum with the time domain provides a more accurate analysis of the structure compared to the frequency domain method. This observed phenomenon is consistent across various results, including average displacement, radians, and average story drift. This accuracy is crucial for a comprehensive understanding of the dynamic performance of the structure, influencing factors such as base shear, base moment, average displacement, radians, and story drift. In summary, the consistent observation of this phenomenon across multiple parameters underscores the effectiveness of the time domain approach in capturing the nuances of structural response.

This research highlights the outcomes of two distinct approaches of RSA and LTHA that are used to assess a specific RC frame structure, based on the seismic wave data from the Kobe 1995 earthquake in Abeno. By comparing two different models, CASE-1 and CASE-2, the research indicates that the natural frequency and fundamental period of the structure are expected to change as the column orientation varies. Consequently, the varying column orientations are also expected to significantly impact the structural performance under seismic loads. This finding is valuable for existing RC frame

structures. Additionally, the seismic analysis conducted on the typical 1980s educational RC frame structure at Kyungpook National University is expected to serve as a valuable reference for reinforcement and maintenance projects for the existing RC buildings.

Although the direction of earthquake loading is generally random, research by Shannon E. Graham, John P. Loveless, and Brendan J. Meade (2018) concludes that the location of earthquakes tends to align with the intersection of tectonic plates. For earthquake situations in the Republic of Korea, Hyunwoo Jee and Sangwhan Han (2019) emphasize the estimated site amplification factor values for the Korean peninsula at each frequency, along with hazard maps for Peak Ground Acceleration. Based on the previous research, the direction of earthquake load can be determined. With the determined direction, designing longer column sections to align with the seismic load direction, based on the position of the construction site, is meaningful for enhancing structural performance under specific seismic loads.

The findings of this research are positioned as a reference not only for new designs but also for reinforcement and maintenance initiatives targeting existing structures. This dual applicability enhances the significance of this research, contributing references that can inform both new construction practices and strategies for preserving older buildings to satisfy contemporary seismic requirements.

REFERENCES

- Cagatay, I. H., Beklen, C., & Mosalam, K. M. (2010). Investigation of short column effect of RC buildings: Failure and prevention. *Computers and Concrete*, 7: 523-532.
- De Angelis, A., Pecce, M., & Rossi, F. (2015). Linear time history analysis for the out-of-plane seismic demand of infill walls in RC framed buildings. *Bulletin of Earthquake Engineering*, 13: 3325-3352.
- Duan, A., Zhao, Z. Z., Chen, J., Qian, J. R., & Jin, W. L. (2014). Nonlinear time history analysis of a pre-stressed concrete containment vessel model under Japan's March 11 earthquake. *Computers and Concrete*, 13: 1-16.
- Estekanchi, H. E., Valamanesh, V., & Vafai, A. (2007). Application of Endurance Time method in linear seismic analysis. *Engineering Structures*, 29: 2551-2562.
- Graham, S. E., Loveless, J. P., & Meade, B. J. (2018). Global Plate Motions and Earthquake Cycle Effects. *Geochemistry, Geophysics, Geosystems*, 19: 2032-2048.
- Jee, H. W., & Han, S. W. (2019). Development of Simulation Model for the 2017 Pohang Earthquake and Construction of Hazard Map based on its Scenario. *Journal of the Korean Society of Hazard Mitigation*, 19: 289-301.
- Kostinakis, K. G., Athanatopoulou, A. M., & Tsiggelis, V. S. (2013). Effectiveness of percentage combination rules for maximum response calculation within the context of linear time history analysis. *Engineering Structures*, 56: 36-45.
- Li, B., Pandey, M. D., Lu, Y., & Dai, K. S. (2019). The Eigenfunction Method for Determining Displacement Time History in Structural Dynamic Analysis. *Periodica Polytechnica Civil Engineering*, 63: 1052-1061.
- Lombardi, L., De Luca, F., & Macdonald, J. (2019). Design of buildings through Linear Time-History Analysis optimising ground motion selection: A case study for RC-MRFs. *Engineering Structures*, 192: 279-295.
- Nguyen, V. Q., Nizamani, Z. A., Park, D., & Kwon, O. S. (2020). Numerical simulation of damage evolution of Daikai station during the 1995 Kobe earthquake. *Engineering Structures*, 206: 110180.
- Okuyama, Y. (2014). Disaster and economic structural change: case study on the 1995 kobe earthquake. *Economic Systems Research*, 26: 98-117.
- Ormeño, M., Larkin, T., & Chouw, N. (2015). Evaluation of seismic ground motion scaling procedures for linear time-history analysis of liquid storage tanks. *Engineering Structures*, 102: 266-277.
- Yusra, A., Mustafa, A., Refiyanni, M., & Zakia, Z. (2023). Performance Structural Analysis of U2C Building with the Kobe Earthquake Spectrum. *International Journal of Engineering, Science & Information Technology*, 3: 36-46.
- (Received May 21, 2024/Revised Jun. 21, 2024/Accepted Jul. 3, 2024)